Passive and Active Materials for Advanced Photonic Integrated Circuitry in Visible and Near-Infrared

Aviad Katiyi and Alina Karabchevsky, School of Electrical and Computer Engineering, Ben-Gurion University of the Negev, Beer-Sheva, Israel

Abstract

Passive and active materials platforms are building blocks of an essential element of photonic integrated circuitry (PIC)-waveguide. Due to their small dimensions, waveguides allow miniaturization and design of efficient optical components on a chip. Therefore, choosing the right material for the waveguide is crucial for photonic integrated circuits. This article overviews passive and active materials for waveguides fabrication and their applications.

Introduction

Materials of photonic integrated circuitry (PIC) dictate the functionality of the circuit (Karabchevsky *et al.*, 2020c). In addition, materials dictate the waveguide wavelengths of operation and its application in terms of passive or active functionality.

Passive materials are materials that transmit the light without absorption or generation or modulation of light. The first passive material offered for guiding light was glass. It is dated back to 1880 when William Wheeler transmitted light through a glass "light pipe". In 1966 the circular fiber with a refractive index higher as compared to its surrounding was first offered as a guiding medium for light transmission (Kao and Hockham, 1966). In 1976 silicon was used for the first time for optical waveguiding.

The development of optics communication gave rise to the development of *active materials* to modulate and amplify the guided light. The first investigated material was lithium niobate ($LiNbO_3$) which is a manmade ferroelectric crystalline material with large electro-optic effect. As the field of integrated photonics evolved, the need for active materials that can generate light has grown accordingly. Semiconductors can be used to generate light. In oppose to lithium niobate, semiconductors have direct bandgap that can be used for light emission. In addition, active materials can be utilized for fabrication of detectors on a chip. Each material group will be elaborated in the next paragraphs.

Passive PIC Materials

Passive materials for PIC are materials that are transparent to light. They do not absorb or emit photons. In **Table 1**, common materials used for passive waveguiding are summarized such as borosilicate glass, silicon, silicon nitride, photonic crystal and polymer. Borosilicate glass has transparency window from ultraviolet (UV) to near-infrared (NIR) with low propagation losses. Silicon transparency window is in NIR and mid-infrared with highest refractive index in optical frequencies. In contrary, photonic crystals operate in short wavelengths range. Below, each material is elaborated.

Glass

Table 2 shows fabrication methods of different types of glass based on either thin film deposition or local modification of the refractive index.

The advantages of using glass is the affordability, a wide range of refractive indices, good transparency, doping possibility and a high threshold to optical damage.

There are two approached to fabricate glass waveguides: local modification and thin film deposition. The local modification is based on locally changing the refractive index of bulk glass. It can be made of various processes such as ion implantation, ion exchange, and UV/femtosecond laser writing. Ion exchange (Karabchevsky and Kavokin, 2016) is an old process that can be dated back to the 5th century when Egyptians used it for coloring glass dices and pots. The ions in the glass (for example Na^+) are replaced with ions from an external source (for example Ag^+ and K^+) usually a salt (Miliou *et al.*, 1989). It is a diffusive process

Table 1 Passive materials

Material	*Refractive index (1.55 μm)*	*Optical window*	*Propagation losses*	*References*
Borosilicate glass	~1.5	0.3–2.5 μm	~0.06 dB/cm (FS written)	(Chen *et al.*, 2018)
Silicon	~3.48	1.2–7 μm	~0.3 dB/cm	(Cardenas *et al.*, 2009)
Silicon nitride	1.6–2	0.4–2.4 μm	~0.3 dB/cm	(Nguyen *et al.*, 1984; Henry *et al.*, 1987)
Photonic crystal	~3.48	$\Delta\lambda$ = 40–50 nm	~0.1 dB/cm	(Notomi *et al.*, 2004)
Polymer	1.3–1.7	0.4–1.6 μm	~0.1 dB/cm	(Eldada and Shacklette, 2000)

Table 2 Fabrication methods of glass waveguides

Method	
Thin film deposition	
Sputtering	* Good quality of the films. * Slow process (few nm per hour) and complex process.
CVD	* Use chemical reactions. * High quality and high performance.
Local Modification	
Ion exchange	* Simple process with low cost. * Hard to accurate determination of their RI profile. * Need to accurate control of the temperature. * Limited materials for substrate and ions.
Ion implantation	* Can use any substrate and any ions. * Defects are created in the substrate.
Femtosecond-Laser Writing	* One step process and maskless that reduce time and cost. * Can by applied on different material. * Fabrication of complex 3D structure

Note: Righini, G.C., Chiappini, A., 2014. Glass optical waveguides: A review of fabrication techniques. Optical Engineering 53 (7), 071819. Hunsperger, R.G., 1995. Integrated Optics, vol. 4. Springer.

that creates graded index change when the higher index is on the glass-salt surface and the index gradually decreases from the surface into the substrate. Each glass and ions have different properties that influence the fabrication and the properties of the waveguide (Findakly, 1985). In 1972, the first waveguide based on ions exchange was made by Tl^{+}-Na^{+} exchange by using borosilicate glass and a mixture of molten nitrate salts (Izawa and Nakagome, 1972). Another method for local index change based ions is ion implantation. In ion implantation, ionized atoms are accelerated using high voltage (up to several MeV) and hit the substrate. The atoms penetrate the substrate, creating a change in the refractive index (as a function of the penetration depth of ions). The advantage of this method, as compared to ions exchange is that any material can be used as a substrate with different ions.

One of the most efficient methods for the fabrication of waveguides (Salter *et al.*, 2012; Huang *et al.*, 2015) is femtosecond writing which was first demonstrated in 1996 (Davis *et al.*, 1996). The substrate is heated by the laser, creating a local change in the refractive index. This method doesn't need a mask for fabrication and can be one-step process. It allows for fabrication of complex 3D structures inside the substrate (Chen and de Aldana, 2014; Grenier *et al.*, 2013).

The other method for the fabrication of glass waveguides is thin film deposition. Instead of modification of the refractive index locally, a layer of glass is deposited on the substrate. A resist is placed on the substrate to create a metal mask. The glass is thermally evaporated on the substrate, creating the waveguide.

Silicon

Silicon is an important material for variety of platforms with applications in photonics, particularly for telecommunications, sensing (Karabchevsky *et al.*, 2020c) and for microelectronic devices. Silicon (Si) has a Diamond crystal structure on a face-centered cubic (fcc) lattice as shown in **Fig. 1**(a). It is cheaper compared to exotic materials such as gallium arsenide (GaAs) and lithium niobate ($LiNbO_3$). In addition, silicon has an energy gap of around 1.1 eV (Chelikowsky and Cohen, 1974) which makes it transparent in the near-IR and preferable for optical telecommunications and overtone spectroscopy (Katiyi and Karabchevsky, 2018, 2020). First silicon waveguide was fabricated back in 1985 (Soref and Lorenzo, 1985). A slab and channel waveguides were fabricated from doped silicon substrate for 1.3 and 1.6 μm wavelengths. The basic platform for silicon waveguides is Silicon-On-Insulator (SOI) wafer which is made of a silicon substrate, silica cladding of 2 μm and silicon guiding layer (200–400 nm typically). SOI wafer can be fabrication of two Si-SiO_2 wafers by Czochralski method and then wafer bonding of the two Si-SiO_2 wafers. In the early 1990s, SOI wafer, which was originally for electronics, was first used for an optical waveguide (Evans *et al.*, 1991; Reed *et al.*, 1992). Silicon waveguide (**Fig. 1**(b)) enables small bending radius for the fundamental mode (Qiu *et al.*, 2014) due to the high index contrast ($n_{Si} \sim 3.45$). This allows fabrication of small structures such as ring resonators (Biberman *et al.*, 2012; Rodriguez *et al.*, 2015) and Mach-Zehnders (Guha *et al.*, 2010; Dong *et al.*, 2012). In addition, silicon is Complementary Metal-Oxide-Semiconductor (CMOS) compatible which allows making hybrid circuit which allows combining electronics and optics (Orcutt *et al.*, 2012; Kita *et al.*, 2018) as shown in **Fig. 1**(c). However, silicon is a centrosymmetric material and, therefore, doesn't have a strong Pockels effect (linear electro-optic effect). As a result, it is hard to perform phase and amplitude modulation. Modulation of light with silicon is possible with for instance the plasma dispersion effect. In 1987, It was shown that by injecting free carriers in silicon and applying voltage one can modulate light in silicon waveguide (Soref and Bennett, 1987). The voltage changes the properties of the doped silicon which in turn changes the effective index of the silicon. However, the modulation in

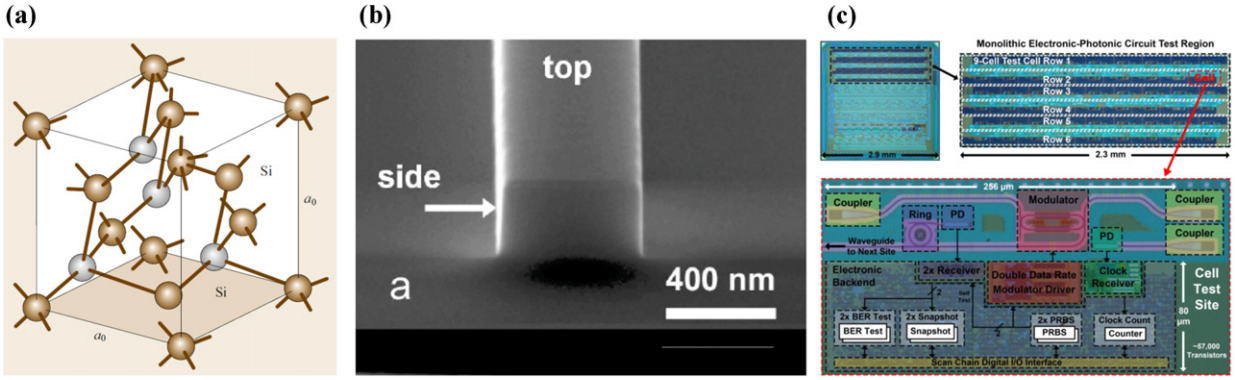

Fig. 1 (a) Crystal structure of Silicon. (b) Scanning electron microscope (SEM) images of a single-mode silicon ridge waveguide. (c) Illustrated micrograph of electronic-photonic integration. Reproduced from (a) Kasap, S., Capper, P., 2017. Springer Handbook of Electronic and Photonic Materials, Springer. (b) Orcutt, J.S., Moss, B., Sun, C., *et al.*, 2012. Open foundry platform for high-performance electronic-photonic integration. Optics Express 20 (11), 12222 –12232. (c) Vlasov, Y.A., McNab, S.J., 2004. Losses in single-mode silicon-on-insulator strip waveguides and bends. Optics Express 12 (8), 1622–1631.

silicon tends to be slow. The main limitation of silicon is that silicon has an indirect band-gap that prevents the fabrication of light sources from native silicon.

Silicon Nitride

Silicon nitride is transparent from 400 to 2400 nm and, therefore, is widely used for passive waveguides. Such waveguides are made from silicon nitride core on silica substrate. In the first step of the fabrication process, a silica cladding is created on the silicon wafer by thermally oxidizing the silicon substrate. The silicon nitride is then grown on the silica using a chemical vapor deposition (CVD) which creates a high-quality layer. Depending on the deposition process, silicon nitride can be silicon-rich (higher refractive index) or nitrogen-rich (lower refractive index). The change in the concentration enables the fabrication of silicon nitride with a range of refractive indices, varying from 1.6 to 1.95 at a wavelength of 632.8 nm (Nguyen *et al.*, 1984). The first fabricated silicon nitride waveguide was a single-mode channel waveguide with propagation losses of 1–2 dB/cm (Boyd *et al.*, 1985). Few years after in 1987, the propagation losses in the communication range was decreased to 0.3 dB/cm (Henry *et al.*, 1987).

Silicon nitride and silicon have their advantages and drawbacks and can be utilized for different applications. The main advantage of silicon nitride is transparency in a wider range from visible to NIR (400–2400 nm). As result, silicon nitride waveguide can be used for Raman spectroscopy on a chip (Zhao *et al.*, 2018) which can not achieve in silicon due to its absorption in the visible. On the other hand, silicon has high index contrast which makes it good for very compact devices. However, the high index contrast ($\Delta = 2$) makes the waveguide sensitive to scattering losses even for a nanometer-scale roughness of the waveguide sidewalls and can exhibit scattering losses of 3–30 dB/cm (Vlasov and McNab, 2004; Lee *et al.*, 2001). The lower index contrast of silicon nitride waveguide decreases the scattering losses but increases the size of the device. Another advantage is that silicon nitride waveguides are fabricated via Low-Pressure Chemical Vapor Deposition (LPCVD) or Plasma-Enhanced Chemical Vapor Deposition (PECVD). These methods allow flexibility in the fabrication process.

Photonic Crystal

It is also important to control light on a nanometer scale. Photonic crystal can guide light in a small-dimensional waveguide via the photonic bandgap (PBG) effect which is graphically presented in **Fig. 2**(a). The photonic bandgap in photonic crystal creates a range of wavelengths that cannot propagate inside the photonic crystal. The photonic crystal is placed in the edges of the guiding layer as shown in **Fig. 2**(b). Photonic crystal occurs when the refractive index changes periodically with a period in order of the λ. The change can occur in one, two or three axes. In 1888, Rayleigh was the first to observe this phenomenon by seeing internal colored reflexion in crystals of chlorate of potash (potassium chlorate – $KclO_3$) (Rayleigh, 1888). He discovered that the color was not due to absorption as the transmission was strictly complementary to the reflection. In 1987, a photonic crystal was first offered for optics applications (Yablonovitch, 1987). Periodic structures were offered for inhibited spontaneous emission to the necessary modes in semiconductor lasers. A few years later, the first experimental photonic crystal was fabricated for microwave region (Yablonovitch *et al.*, 1991). A face-centered-cubic (fcc) structure was made by drilling holes into a dielectric material to create a 3D photonic crystal for high-Q electromagnetic cavities.

One of the conventional configurations for waveguides is a 2D photonic crystal made of silicon. Two-dimensional photonic crystal can be fabricated by drilling holes in a material using e-beam lithography or by placing rods in air. Waveguide based on photonic crystal has few advantages compared to the conventional waveguide. Guiding light using photonic band-gap has lower bend-losses compared to total internal reflection. It allows for a smaller bend with low loss (Liu and Fan, 2013; Zhao *et al.*, 2015)

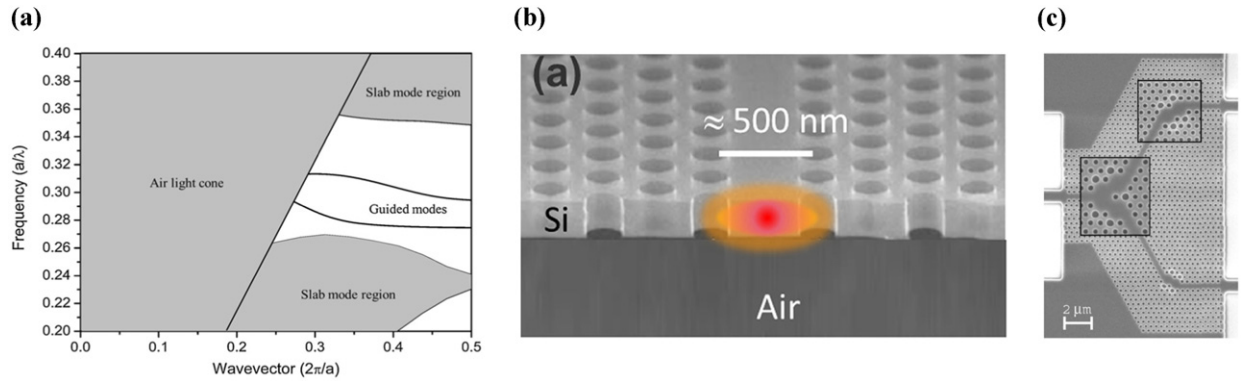

Fig. 2 (a) Dispersion diagram of the photonic crystal waveguide. (b) Photonic crystal waveguide. (c) Scanning electron micrograph of photonic crystal splitter. Reproduced from (a) Dutta, H.S., Goyal, A.K., Srivastava, V., Pal, S., 2016. Coupling light in photonic crystal waveguides: A review. Photonics and Nanostructures-Fundamentals and Applications 20, 41–58. (b) Frandsen, L.H., Borel, P.I., Y., Zhuang, *et al.*, 2004. Ultralow-loss 3-db photonic crystal waveguide splitter. Optics Letters 29 (14), 1623–1625. (c) Lalanne, P., Coudert, S., Duchateau, G., Dilhaire, S., Vynck, K., 2018. Structural slow waves: Parallels between photonic crystals and plasmonic waveguides. ACS Photonics 6 (1), 4–17.

that can be utilized for compact y-splitter (Frandsen *et al.*, 2004). An interesting phenomenon in a photonic crystal is a slow light phenomenon that reduces the group velocity of the light by optical resonances of the guiding material. It allows stronger light-matter interaction, (Mahmoodian *et al.*, 2017) a stronger non-linear process for unit length (Ek *et al.*, 2014) and can also be used for a sharper waveguide bend (Zhao *et al.*, 2015).

Polymers

Polymers are easy to fabricate. The fabrication process of polymer waveguides is much more simple compared to other materials which make polymer waveguides so affordable. Furthermore, the refractive index of polymers is easy to tune. It can vary from 1.3 to 1.7. Polymers can have different properties; one can be glossy while the other can be flexible (Kim *et al.*, 2010). The optical losses are generally in order of tenths of dB/cm at the telecommunications windows wavelength (Eldada and Shacklette, 2000). For these reasons, polymer waveguides are ideal replacement to glass waveguide for cheap, robust and mass production. In the 1970s, polymer was first used for guiding light in thin-film (Harris *et al.*, 1970). The thin films were made of polyester and polyurethane epoxy resins and the light was coupled by a prism. Polymers can also be used for active waveguides due to the possibility of having large thermo-optic (TO) (Zhang *et al.*, 2006) and electro-optic (EO) (Wu *et al.*, 2012) coefficients.

The common methods for producing polymer films are spin coating and extrusion. Each method has advantages and disadvantages. Spin-coating, for instance, has good control of the thickness and uniformity; on the other hand, film striation is difficult. For patterning the polymer films, few methods can be used such as photoresist based pattering and direct lithographic patterning. The major advantage of polymers waveguide is that the fabrication process can be made by imprinting technique which can overcome the diffraction limitation of photolithography. This technique was initiated in the 1990s (Chou *et al.*, 1996) and can be an alternative to UV optical lithography, ranging from the nanometer to millimeter scale. This method is based on creating a mold and reverse replica of the mold on a polymer layer. It can be formed by pressing hot polymer (thermal imprinting technique) or by UV curing of liquid polymer (UV imprinting technique). Imprinting technique can be used for passive device, such as microring resonator, (Girault *et al.*, 2015; Wei and Krishnaswamy, 2017) waveguide grating (Yang *et al.*, 2015; Prokop *et al.*, 2016) and microlens (Ahmed *et al.*, 2017; Jung and Jeong, 2015).

Active PIC Materials

The ability to perform modulation is very important in integrated photonics. The demand for active material waveguides is back in 1960s when the evolution of optical fiber required the modulation and amplification of the signal. As compared to above mention materials, materials discussed in this section have non-linear electooptic effect with second-order Kerr nonlinearity (χ^2) or linear (Pockels) electro-optic effect due to their molecular structure and can be used to modulate or amplify the light. **Table 3** shows the properties of common material for active waveguides.

Lithium Niobate

The first investigated and the most popular material for active waveguides in integrated photonics is lithium niobate ($LiNbO_3$). Lithium niobate is a manmade ferroelectric crystalline material with transparency in a wide range (0.4–5 μm). In 1965, lithium niobate was first grown using Czochralski technique (Ballman, 1965) while the first integrated waveguide was fabricated in 1974

Table 3 Active materials

Material	*Refractive index*	$r_{33}\left[\frac{pm}{V}\right]$	$d_{33}\left[\frac{pm}{V}\right]$	$\chi^{(3)}\left[\frac{cm^2}{W}\right]$	*Emission*
Lithium niobate	~2.2	30 (Abouellell and Leonberger, 1989)	27 (Chang *et al.*, 2017)	5.3×10^{-15} (Chang *et al.*, 2018)	none
Gallium arsenide	~3.6	1.43 (Wu and Zhang, 1996)	119 (Chang *et al.*, 2018)	1.6×10^{-13} (Chang *et al.*, 2018)	0.6–1.7 μm

by metal-diffusion process, forming low-loss TE and TM mode optical waveguides (Schmidt and Kaminow, 1974). In contrast to silicon and silicon nitride, lithium niobate have strong electro-optic coefficient ($r_{33} = 30$pm/V (Abouellell and Leonberger, 1989)) and high second-order nonlinear coefficient ($d_{33} = 27$pm/V (Chang *et al.*, 2017)). Therefore, it can be utilized for active waveguides. The strong electro-optic coefficient allows utilizing lithium niobate in optical modulators (Wang *et al.*, 2018a,b). Furthermore, its response time is much shorter compared to silicon modulators (femtoseconds vs. nanoseconds). Due to the large second- and third-order nonlinearity, lithium niobate waveguides are also very attractive for non-linear applications. It can be used for second- and third-order nonlinear processes such as second harmonic generation (SHG), (Wang *et al.*, 2017) supercontinuum generation (SCG) (Yu *et al.*, 2019) and sum-frequency generation (SFG) (Ye *et al.*, 2020). It also exhibits strong piezoelectric effect and photoelectric properties (Weis and Gaylord, 1985) which can be utilized for acousto-optic modulation (Cai *et al.*, 2019).

The simple platform for integrated photonics is lithium niobate on insulator (LNOI). LNOI wafers are fabricated by ion slicing process which is commonly used for SOI wafers. Integration of lithium niobate into silicon allows fabrication of active components on SOI wafer. This can be done by ion splicing of lithium niobate to a silicon wafer (Rabiei and Gunter, 2004) and can be used for resonators and modulators. However, it is less efficient due to the index difference between silicon (~3.48) to lithium niobate (~2.14) which decreases the confinement in the LN and the absorption of silicon in $\lambda < 1.1\mu$m. A much efficient method is integration of lithium niobate with silicon nitride (Chang *et al.*, 2017). Silicon nitride has lower material loss, broad transparency and doesn't suffer from two photons absorption.

III-V Ternary and Quaternary Alloys

A material that can be used for creating a light source on a chip is a semiconductor. Semiconductors have a direct bandgap that enables emitting or amplifying the light as illustrated in **Fig. 3**(a-b). In 1962, the first laser emission from GaAs junction was observed and reported in refs. (Hall *et al.*, 1962; Quist *et al.*, 1962). Semiconductors have few advantages: monolithic integration with optoelectronic and electronic devices, suitable for high-speed low-drive voltage modulators and switches and controllable fabrication processes.

The first and mainly used semiconductors for optoelectronic devices are III-V compounds such as GaAs and InP. III-V semiconducting compound alloys are made from Group III (Al, Ga, In) and group V (N, P, As, Sb) atoms. The ability to tune the bandgap, make III-V semiconductor alloys very attractive for waveguides. By changing the concentration of the atoms, the bandgap energy (E_g) and lattice parameter (a) can be changed (**Fig. 3**(c)), creating different light sources and detectors (Karabchevsky, 2020) from the same material on the same substrate. Therefore, semiconductor alloys can be used for light emitting diodes, laser diodes and photodetectors, allowing monolithic integration of them on a chip. However, the more interesting features of semiconductors alloys are ternary (for example gallium aluminum arsenide $Al_xGa_{1-x}As$) and quaternary (for example Indium gallium arsenide phosphide $In_xGa_{1-x}As_yP_{1-y}$) alloys. The number of compounds in the alloys (three or four) change the properties of the alloy. In ternary alloys, the bandgap energy and lattice parameter cannot be changed separately while in quaternary alloy it is possible. The common for non-linear optics are gallium arsenide (GaAs) and aluminum gallium arsenide (AlGaAs) due to their high second-order ($\chi^{(2)}$) and third-order ($\chi^{(3)}$) nonlinear optical coefficients (Chang *et al.*, 2018). By using GaAs on SOI with Silica cladding, the second-harmonic efficiency can increase to 13000% $W^{-1}cm^{-2}$ (Chang *et al.*, 2018).

Dielectric and Plasmonic Overlayers

A side effect of the total internal reflection is the evanescent field. Due to the evanescent field beyond the guiding layer, an overlayer can be placed on the guiding layer to tune the guided mode.

Metallic Overlayer

Surface plasmon polaritons (SPPs) are electromagnetic waves that propagate in the interface between metal and dielectric as shown in **Fig. 4**(a). Surface plasmon was first observed by Wood in 1902 (Wood, 1902). He found a strange feature in the reflection of metallic grating with an absorption band. In 1959, Pines described these losses, attributed them to the oscillations of free electrons and called the oscillations "plasmons" (Pines, 1956). In the same year, Fano gave them the term "polariton" (Fano, 1956). In 1959, it was first observed in non-opaque aluminum films (Turbadar, 1959). The reflectance as a function of the angle of aluminum films evaporated on a glass substrate was investigated. For a certain range of aluminum thicknesses, a drop in the reflectance was observed after the critical angle for p-polarization (parallel - TM mode) wave. Later,

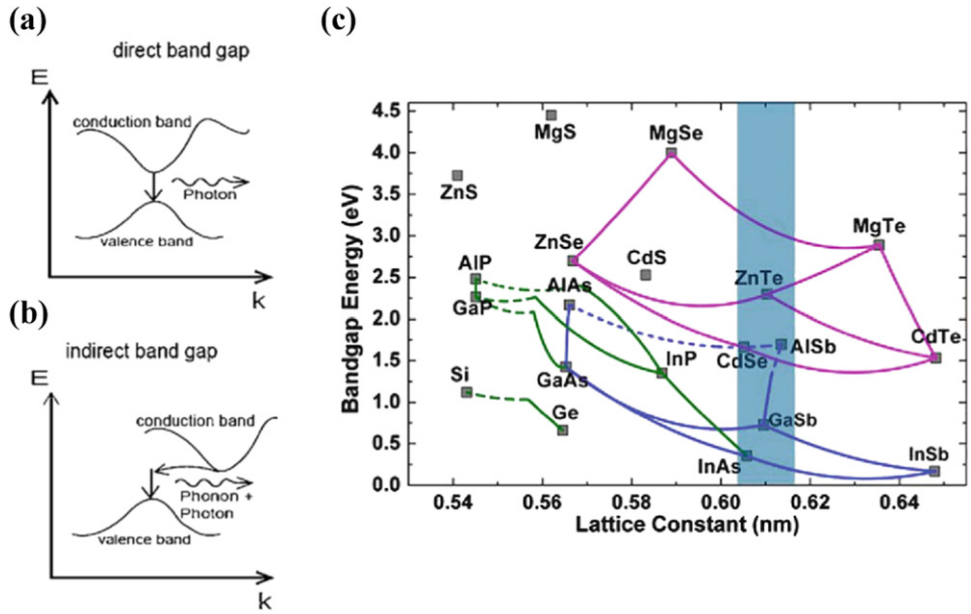

Fig. 3 Energy band structures and photon generation in (a) direct and (b) indirect band gap semiconductors and (c) band gap energy of III-V and II-VI semiconductors (full line - direct band gap. dashed line - indirect band gap.). Reproduced from Tong, X.C., 2014. Advanced Materials for Integrated Optical Waveguides 46 Springer.

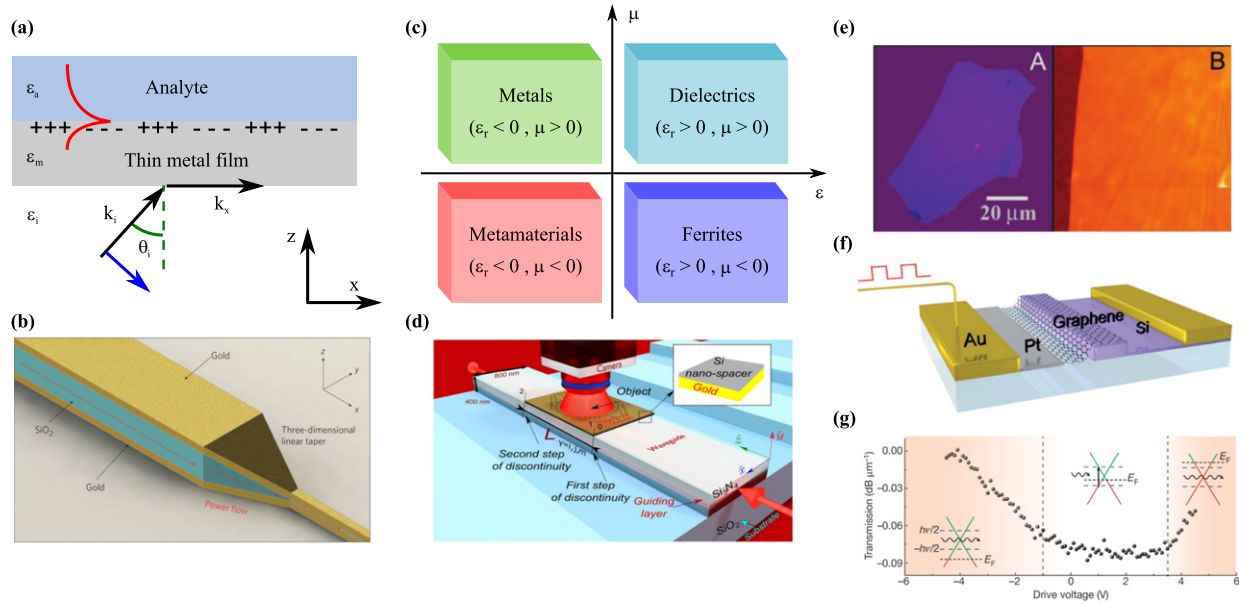

Fig. 4 (a) Illustration of plasmon excitation. (b) A schematic illustration of a three-dimensional metal-insulator-metal (MIM) nanoplasmonic photon compressor (3D NPC). Reproduced from (Choo *et al.*). (c) Schematics of materials characterization by electric permittivity (ε) and magnetic permeability (μ). (d) Illustration of the composite waveguide structure and materials for the invisibility cloaking. (e) (left) Photograph of a relatively large multilayer graphene and (right) atomic force microscope (AFM) near its edge. (f) Illustartion of a graphene based waveguide optical modulator and (g) electro-optical response of the device at different drive voltages (f) and (g). Reproduced from (b) Choo, H., Kim, M.-K., Staffaroni, M., *et al.*, 2012. Nanofocusing in a metal-insulator-metal gap plasmon waveguide with a three-dimensional linear taper Nature Photonics 6 (12), 838–844. (d) Galutin, Y., Falek, E., Karabchevsky, A., 2017. Invisibility cloaking scheme by evanescent fields distortion on composite plasmonic waveguides with si nano-spacer. Scientific Reports 7 (1), 1–8. (e) Novoselov, K.S., Geim, A.K., Morozov, S.V., *et al.*, 2004. Electric field effect in atomically thin carbon films. Science 306 (5696), 666–669. (g) Liu, M., Yin, X., Ulin-Avila, E., *et al.*, 2011. A graphene-based broadband optical modulator. Nature 474 (7349), 64–67.

Otto and Kretschmann offered optical excitation for surface plasmons on a metal film (Otto, 1968; Kretschmann and Raether, 1968) using a prism as a coupling medium for the excitation of plasmons. In 1974, the term 'surface plasmon polariton' (SPP) was introduced to the oscillations of free electrons (Cunningham *et al.*, 1974). Later, it was shown that plasmons are not limited to bulk metal but can be also localized in silver and gold nanoparticles (Kreibig and Zacharias, 1970). These plasmons are called localized surface plasmon resonance (LSPR). Localized surface plasmon resonance occurs when the metal has a sub-wavelength structure unit and the plasmons are localized. As a result, the light is concentrated in a sub-wavelength point that is smaller than the wavelength. It gives the possibility of fabrication a nanoscale photonic circuit.

A metal thin layer can be placed on a waveguide and be used for a variety of applications. The plasmon resonance is sensitive to the environment and the changes in the refractive index of the surrounding cause a shift in the plasmon. The shift can be used for sensors (Ji *et al.*, 2017; Krupin *et al.*, 2013; Karabchevsky *et al.*, 2015). By applying bias on the metal layer, plasmonic waveguides can act as high speed modulators (Melikyan *et al.*, 2014; Haffner *et al.*, 2015). In addition, surface plasmon polaritons can overcome the diffraction limit and propagate in nanoscale dimensions. For example, by using a metal-insulator-metal (MIM) waveguide (**Fig. 4**(b)), the plasmons can be used for nanofocusing on sub-wavelength point (Choo *et al.*, 2012). Metal can be also implemented on waveguides by nanorods or nanoparticles, which acts as LSPR. It can be used as nanoantenna to tune the functionality of waveguide, (Guo *et al.*, 2017; Karabchevsky *et al.*, 2020b) to enhance quantum-dots light emission (Abass *et al.*, 2014) and for enhanced sensing (Wuytens *et al.*, 2017; Chamanzar *et al.*, 2013; Karabchevsky *et al.*, 2018).

Metamaterial Overlayer

Metamaterials have a growing interest in the past decade. The word metamaterial was first used in 2001 by Lakhtakia *et al.* (2001) to describe artificial material with anomalous electromagnetic properties (meta meaning is beyond). A metamaterial is a human-made material that can have special properties that do not exist in natural materials. Important parameters that define the material TYPE are the permittivity (ε) and the permeability (μ) as shown in **Fig. 4**(c). The main concept of metamaterial is based on the change in the electric and magnetic dipole moments in the inclusions. The resonant changes the permittivity and the permeability of the medium which can be described by Lorentz classical theory. Metamaterials can have negative permittivity and permeability (Zhang *et al.*, 2005) which does not exist in nature. By having a negative real part of the permittivity and the permeability, it creates a negative index material (NIM) (also called double-negative (DNG) material) which can be used for the fabrication of a perfect lens that overcomes the diffraction limit (Pendry, 2000). In negative index material, the electric field, the magnetic field and the propagation direction follow the left-hand rule (for this reason it is also called left-handed material - LHM). A Metamaterial can also have low values (between -1 and 1) or extremely high values of permittivity and/or permeability (Alù *et al.*, 2007).

The first metamaterial, artificial chiral molecule, was fabricated by Bose in 1898 (Bose, 1898). He found that the twisted structure of the jute creates a twist of the plane of polarization. Metamaterials can be implemented on a waveguide mainly used in the two-dimensional configuration, called as meta-surface. It can be made from dielectric, metal and even from the waveguide itself. It can be used for optical cloaking (Galutin *et al.*, 2017) (**Fig. 4**(d)), anti-reflection structure (Karabchevsky *et al.*, 2020a; Falek *et al.*, 2021) and to enhanced the spontaneous emission (Roth *et al.*, 2017).

Graphene Overlayer

Also 2D materials like graphene has a growing interest in integrated photonics. Graphene is a single atomic layer honeycomb of carbon (2D) that can be separated from graphite. Graphite is hexagonal pattern layers of carbon atoms hold by a weak van der Waals force between the adjacent layers (Charlier *et al.*, 1994). Graphite has good thermal and electric conductivity in the layers and poor between them due to the bonding behavior. Therefore, a thin layer of graphite was considered as a good replacement for metal to miniaturize metallic components. The leap in graphene research was in 2004 when a single layer of graphene was first isolated from graphite (Novoselov *et al.*, 2004). By using mechanical exfoliation, few layers of graphite and even a single layer of graphite (graphene) were separated as shown in **Fig. 4**(e). This discovery opened the field of graphene based devices.

Graphene has few unique properties. Graphene has high electron-mobility ($2.5\ 10^5\ cm^{-2}\ V^{-1}\ s^{-1}$ – 4 times higher than III-V semiconductors (Xia *et al.*, 2009)) and therefore, it can be used for high-speed modulators (Ye *et al.*, 2016; Kovacevic *et al.*, 2018; Gao *et al.*, 2015). It can be used for making modulators from passive materials by placing graphene on the guiding layer of passive waveguide such as silicon and silicon nitride (Liu *et al.*, 2011; Phare *et al.*, 2015). By applying voltage, the Fermi level of graphene is changed and tune the optical properties of the graphene layer, creates modulation (Ansell *et al.*, 2015; Ding *et al.*, 2017) as shown in **Fig. 4**(f-g). The same configuration with the high mobility can be used for high-speed photodetectors (Guo *et al.*, 2020) which can even operate at zero dark current (Muench *et al.*, 2019). The advantage of graphene based photodetector is that they are not spectrally limited (Mueller *et al.*, 2010) as compared to germanium (Ge) photodetectors due to the broadband optical absorption of graphene. A graphene layer has been proposed as an alternative for plasmonics due to the much tighter confinement (Chen *et al.*, 2012) and the ability to be electrically tunable (Chen *et al.*, 2012; Fei *et al.*, 2012).

Summary and Outlook

To conclude, optical waveguides can be used for variety of applications thanks to the development of waveguide materials and the fabrication processes. Optical waveguides can be made from active and passive materials which allow fabrication of passive devices for signal transmission and active devices for light generation, absorption or modulation. Different materials and waveguide's architecture will dictate the application to be demonstrated. Further research in both passive and active materials may allow the fabrication of novel waveguides with novel functionalities.

References

Abass, A., Rodriguez, S.R.-K., Ako, T., *et al.*, 2014. Active liquid crystal tuning of metallic nanoantenna enhanced light emission from colloidal quantum dots. Nano Letters 14 (10), 5555–5560.

Abouellell, M.M., Leonberger, F.J., 1989. Waveguides in lithium niobate. Journal of the American Ceramic Society 72 (8), 1311–1321.

Ahmed, R., Yetisen, A.K., Butt, H., 2017. High numerical aperture hexagonal stacked ring-based bidirectional flexible polymer microlens array. ACS Nano 11 (3), 3155–3165.

Alù, A., Engheta, N., Erentok, A., Ziolkowski, R.W., 2007. Single-negative, double-negative, and low-index metamaterials and their electromagnetic applications. IEEE Antennas and Propagation Magazine 49 (1), 23–36.

Ansell, D., Radko, I., Han, Z., *et al.*, 2015. Hybrid graphene plasmonic waveguide modulators. Nature Communications 6 (1), 1–6.

Ballman, A.A., 1965. Growth of piezoelectric and ferroelectric materials by the czochraiski technique. Journal of the American Ceramic Society 48 (2), 112–113.

Biberman, A., Shaw, M.J., Timurdogan, E., Wright, J.B., Watts, M.R., 2012. Ultralow-loss silicon ring resonators. Optics Letters 37 (20), 4236–4238.

Bose, J.C., 1898. On the rotation of plane of polarisation of electric wave by a twisted structure. Proceedings of the Royal Society of London 63 (389–400), 146–152.

Boyd, J., Wu, R., Zelmon, D., *et al.*, 1985. Planar and channel optical waveguides utilizing silicon technology. In: Integrated Optical Circuit Engineering I, vol. 517. International Society for Optics and Photonics. pp. 100–105.

Cai, L., Mahmoud, A., Khan, M., *et al.*, 2019. Acousto-optical modulation of thin film lithium niobate waveguide devices. Photonics Research 7 (9), 1003–1013.

Cardenas, J., Poitras, C.B., Robinson, J.T., *et al.*, 2009. Low loss etchless silicon photonic waveguides. Optics Express 17 (6), 4752–4757.

Chamanzar, M., Xia, Z., Yegnanarayanan, S., Adibi, A., 2013. Hybrid integrated plasmonic-photonic waveguides for on-chip localized surface plasmon resonance (lspr) sensing and spectroscopy. Optics Express 21 (26), 32086–32098.

Chang, L., Pfeiffer, M.H., Volet, N., *et al.*, 2017. Heterogeneous integration of lithium niobate and silicon nitride waveguides for wafer-scale photonic integrated circuits on silicon. Optics Letters 42 (4), 803–806.

Chang, L., Boes, A., Guo, X., *et al.*, 2018. Heterogeneously integrated gaas waveguides on insulator for efficient frequency conversion. Laser & Photonics Reviews 12 (10), 1800149.

Charlier, J.-C., Gonze, X., Michenaud, J.-P., 1994. Graphite interplanar bonding: electronic delocalization and van der waals interaction. Europhysics Letters) 28 (6), 403.

Chelikowsky, J.R., Cohen, M.L., 1974. Electronic structure of silicon. Physical Review B 10 (12), 5095.

Chen, F., de Aldana, J.V., 2014. Optical waveguides in crystalline dielectric materials produced by femtosecond-laser micromachining. Laser & Photonics Reviews 8 (2), 251–275.

Chen, G.Y., Piantedosi, F., Otten, D., *et al.*, 2018. Femtosecond-laser-written microstructured waveguides in bk7 glass. Scientific Reports 8 (1), 1–7.

Chen, J., Badioli, M., Alonso-González, P., *et al.*, 2012. Optical nano-imaging of gate-tunable graphene plasmons. Nature 487 (7405), 77–81.

Choo, H., Kim, M.-K., Staffaroni, M., *et al.*, 2012. Nanofocusing in a metal-insulator-metal gap plasmon waveguide with a three-dimensional linear taper. Nature Photonics 6 (12), 838.

Chou, S.Y., Krauss, P.R., Renstrom, P.J., 1996. Imprint lithography with 25-nanometer resolution. Science 272 (5258), 85–87.

Cunningham, S., Maradudin, A., Wallis, R., 1974. Effect of a charge layer on the surface-plasmon-polariton dispersion curve. Physical Review B 10 (8), 3342.

Davis, K.M., Miura, K., Sugimoto, N., Hirao, K., 1996. Writing waveguides in glass with a femtosecond laser. Optics Letters 21 (21), 1729–1731.

Ding, Y., Guan, X., Zhu, X., *et al.*, 2017. Efficient electro-optic modulation in low-loss graphene-plasmonic slot waveguides. Nanoscale 9 (40), 15576–15581.

Dong, P., Chen, L., Chen, Y.-k., 2012. High-speed low-voltage single-drive push-pull silicon mach-zehnder modulators. Optics Express 20 (6), 6163–6169.

Ek, S., Lunnemann, P., Chen, Y., *et al.*, 2014. Slow-light-enhanced gain in active photonic crystal waveguides. Nature Communications 5 (1), 1–8.

Eldada, L., Shacklette, L.W., 2000. Advances in polymer integrated optics. IEEE Journal of Selected Topics in Quantum Electronics 6 (1), 54–68.

Evans, A., Hall, D., Maszara, W., 1991. Propagation loss measurements in silicon-on-insulator optical waveguides formed by the bond-and-etchback process. Applied Physics Letters 59 (14), 1667–1669.

Falek, E., Katiyi, A., Greenberg, Y., Karabchevsky, A., 2021. On-chip metasurface-on-facets for ultra-high transmission through waveguides in near-infrared. Advanced Optical Materials 9 (11).

Fano, U., 1956. Atomic theory of electromagnetic interactions in dense materials. Physical Review 103 (5), 1202.

Fei, Z., Rodin, A., Andreev, G.O., *et al.*, 2012. Gate-tuning of graphene plasmons revealed by infrared nano-imaging. Nature 487 (7405), 82–85.

Findakly, T., 1985. Glass waveguides by ion exchange: A review. Optical Engineering 24 (2), 242244.

Frandsen, L.H., Borel, P.I., Zhuang, Y., *et al.*, 2004. Ultralow-loss 3-db photonic crystal waveguide splitter. Optics Letters 29 (14), 1623–1625.

Galutin, Y., Falek, E., Karabchevsky, A., 2017. Invisibility cloaking scheme by evanescent fields distortion on composite plasmonic waveguides with si nano-spacer. Scientific Reports 7 (1), 1–8.

Gao, Y., Shiue, R.-J., Gan, X., *et al.*, 2015. High-speed electro-optic modulator integrated with graphene-boron nitride heterostructure and photonic crystal nanocavity. Nano Letters 15 (3), 2001–2005.

Girault, P., Lorrain, N., Poffo, L., *et al.*, 2015. Integrated polymer micro-ring resonators for optical sensing applications. Journal of Applied Physics 117 (10), 104504.

Grenier, J.R., Fernandes, L.A., Herman, P.R., 2013. Femtosecond laser writing of optical edge filters in fused silica optical waveguides. Optics Express 21 (4), 4493–4502.

Guha, B., Gondarenko, A., Lipson, M., 2010. Minimizing temperature sensitivity of silicon mach-zehnder interferometers. Optics Express 18 (3), 1879–1887.

Guo, J., Li, J., Liu, C., *et al.*, 2020. High-performance silicon- graphene hybrid plasmonic waveguide photodetectors beyond 1.55 μm. Light: Science & Applications 9 (1), 1–11.

Guo, R., Decker, M., Setzpfandt, F., *et al.*, 2017. High-bit rate ultra-compact light routing with mode-selective on-chip nanoantennas. Science Advances 3 (7), e1700007.

Haffner, C., Heni, W., Fedoryshyn, Y., *et al.*, 2015. All-plasmonic mach-zehnder modulator enabling optical high-speed communication at the microscale. Nature Photonics 9 (8), 525–528.

Hall, R.N., Fenner, G.E., Kingsley, J., Soltys, T., Carlson, R., 1962. Coherent light emission from GaAs junctions. Physical Review Letters 9 (9), 366.

Harris, J., Shubert, R., Polky, J., 1970. Beam coupling to films. JOSA 60 (8), 1007–1016.

Henry, C.H., Kazarinov, R.F., Lee, H.J., Orlowsky, K.J., Katz, L., 1987. Low loss si_3n_4-sio 2 optical waveguides on si. Applied Optics 26 (13), 2621–2624.

Huang, L., Salter, P., Karpiński, M., *et al.*, 2015. Waveguide fabrication in kdp crystals with femtosecond laser pulses. Applied Physics A 118 (3), 831–836.

Izawa, T., Nakagome, H., 1972. Optical waveguide formed by electrically induced migration of ions in glass plates. Applied Physics Letters 21 (12), 584–586.
Ji, L., Sun, X., He, G., *et al.*, 2017. Surface plasmon resonance refractive index sensor based on ultraviolet bleached polymer waveguide. Sensors and Actuators B: Chemical 244, 373–379.
Jung, H., Jeong, K.-H., 2015. Monolithic polymer microlens arrays with high numerical aperture and high packing density. ACS Applied Materials & Interfaces 7 (4), 2160–2165.
Kao, K., Hockham, G.A., 1966. Dielectric-fibre surface waveguides for optical frequencies. Proceedings of the Institution of Electrical Engineers vol. 113, 1151–1158. (IET).
Karabchevsky, A., 2020. On-chip optical vortex-based nanophotonic detectors. Light, Science & Applications 9.
Karabchevsky, A., Kavokin, A., 2016. Giant absorption of light by molecular vibrations on a chip. Scientific Reports 6 (1), 1–7.
Karabchevsky, A., Wilkinson, J.S., Zervas, M.N., 2015. Transmittance and surface intensity in 3d composite plasmonic waveguides. Optics Express 23 (11), 14407–14423.
Karabchevsky, A., Falek, E., Greenberg, Y., *et al.*, 2020a. Broadband transparency with all-dielectric metasurfaces engraved on silicon waveguide facets: Effect of inverted and extruded features based on babinet's principle. Nanoscale Advances 2 (7), 2977–2985.
Karabchevsky, A., Hazan, A., Dubavik, A., 2020b. All-optical polarization-controlled nanosensor switch based on guided-wave surface plasmon resonance via molecular overtone excitations in the near-infrared. Advanced Optical Materials 8 (19), 2000769.
Karabchevsky, A., Katiyi, A., Ang, A.S., Hazan, A., 2020c. On-chip nanophotonics and future challenges. Nanophotonics 9 (12), 3733–3753.
Karabchevsky, A., Katiyi, A., Bin Abdul Khudus, M.I.M., Kavokin, A.V., 2018. Tuning the near-infrared absorption of aromatic amines on tapered fibers sculptured with gold nanoparticles. ACS Photonics 5 (6), 2200–2207.
Katiyi, A., Karabchevsky, A., 2018. Si nanostrip optical waveguide for on-chip broadband molecular overtone spectroscopy in near-infrared. ACS Sensors 3 (3), 618–623.
Katiyi, A., Karabchevsky, A., 2020. Deflected talbot-mediated overtone spectroscopy in near-infrared as a label-free sensor on a chip. ACS Sensors 5 (6), 1683–1688.
Kim, K.-J., Kim, J.-W., Oh, M.-C., Noh, Y.-O., Lee, H.-J., 2010. Flexible polymer waveguide tunable lasers. Optics Express 18 (8), 8392–8399.
Kita, D.M., Miranda, B., Favela, D., *et al.*, 2018. High-performance and scalable on-chip digital fourier transform spectroscopy. Nature Communications 9 (1), 1–7.
Kovacevic, G., Phare, C., Set, S.Y., Lipson, M., Yamashita, S., 2018. Ultra-high-speed graphene optical modulator design based on tight field confinement in a slot waveguide. Applied Physics Express 11 (6), 065102.
Kreibig, U., Zacharias, P., 1970. Surface plasma resonances in small spherical silver and gold particles. Zeitschrift für Physik A Hadrons and Nuclei 231 (2), 128–143.
Kretschmann, E., Raether, H., 1968. Radiative decay of non-radiative surface plasmons excited by light. Zeitschrift für Naturforschung A 23 (12), 2135–2136.
Krupin, O., Asiri, H., Wang, C., Tait, R.N., Berini, P., 2013. Biosensing using straight long-range surface plasmon waveguides. Optics Express 21 (1), 698–709.
Lakhtakia, A., Weiglhofer, W.S., Hodgkinson, I.J., 2001. Complex Mediums II: Beyond Linear Isotropic Dielectrics. 4467. SPIE.
Lee, K.K., Lim, D.R., Kimerling, L.C., Shin, J., Cerrina, F., 2001. Fabrication of ultralow-loss si/sio 2 waveguides by roughness reduction. Optics Letters 26 (23), 1888–1890.
Liu, M., Yin, X., Ulin-Avila, E., *et al.*, 2011. A graphene-based broadband optical modulator. Nature 474 (7349), 64–67.
Liu, V., Fan, S., 2013. Compact bends for multi-mode photonic crystal waveguides with high transmission and suppressed modal crosstalk. Optics Express 21 (7), 8069–8075.
Mahmoodian, S., Prindal-Nielsen, K., Söllner, I., Stobbe, S., Lodahl, P., 2017. Engineering chiral light-matter interaction in photonic crystal waveguides with slow light. Optical Materials Express 7 (1), 43–51.
Melikyan, A., Alloatti, L., Muslija, A., *et al.*, 2014. High-speed plasmonic phase modulators. Nature Photonics 8 (3), 229–233.
Miliou, A., Zhenguang, H., Cheng, H., Srivastava, R., Ramaswamy, R.V., 1989. Fiber-compatible k^+-na^+ ion-exchanged channel waveguides: fabrication and characterization. IEEE Journal of Quantum Electronics 25 (8), 1889–1897.
Mueller, T., Xia, F., Avouris, P., 2010. Graphene photodetectors for high-speed optical communications. Nature Photonics 4 (5), 297–301.
Muench, J.E., Ruocco, A., Giambra, M.A., *et al.*, 2019. Waveguide-integrated, plasmonic enhanced graphene photodetectors. Nano Letters 19 (11), 7632–7644.
Nguyen, V., Burton, S., Pan, P., 1984. The variation of physical properties of plasma-deposited silicon nitride and oxynitride with their compositions. Journal of the Electrochemical Society 131 (10), 2348.
Notomi, M., Shinya, A., Mitsugi, S., Kuramochi, E., Ryu, H., 2004. Waveguides, resonators and their coupled elements in photonic crystal slabs. Optics Express 12 (8), 1551–1561.
Novoselov, K.S., Geim, A.K., Morozov, S.V., *et al.*, 2004. Electric field effect in atomically thin carbon films. Science 306 (5696), 666–669.
Orcutt, J.S., Moss, B., Sun, C., *et al.*, 2012. Open foundry platform for high-performance electronic-photonic integration. Optics Express 20 (11), 12222–12232.
Otto, A., 1968. Excitation of nonradiative surface plasma waves in silver by the method of frustrated total reflection. Zeitschrift für Physik A Hadrons and Nuclei 216 (4), 398–410.
Pendry, J.B., 2000. Negative refraction makes a perfect lens. Physical Review Letters 85 (18), 3966.
Phare, C.T., Lee, Y.-H.D., Cardenas, J., Lipson, M., 2015. Graphene electro-optic modulator with 30 ghz bandwidth. Nature Photonics 9 (8), 511–514.
Pines, D., 1956. Collective energy losses in solids. Reviews of Modern Physics 28 (3), 184.
Prokop, C., Schoenhardt, S., Laegel, B., *et al.*, 2016. Air-suspended su-8 polymer waveguide grating couplers. Journal of Lightwave Technology 34 (17), 3966–3971.
Qiu, C., Sheng, Z., Li, H., *et al.*, 2014. Fabrication, characterization and loss analysis of silicon nanowaveguides. Journal of Lightwave Technology 32 (13), 2303–2307.
Quist, T.M., Rediker, R.H., Keyes, R., *et al.*, 1962. Semiconductor maser of gaas. Applied Physics Letters 1 (4), 91–92.
Rabiei, P., Gunter, P., 2004. Optical and electro-optical properties of submicrometer lithium niobate slab waveguides prepared by crystal ion slicing and wafer bonding. Applied Physics Letters 85 (20), 4603–4605.
Rayleigh, L., 1888. Xxvi. on the remarkable phenomenon of crystalline reflexion described by prof. stokes. The London, Edinburgh, and Dublin Philosophical Magazine and Journal of Science 26 (160), 256–265.
Reed, G., Jinhua, L., Tang, C., *et al.*, 1992. Silicon on insulator optical waveguides formed by direct wafer bonding. Materials Science and Engineering: B 15 (2), 156–159.
Rodriguez, G.A., Hu, S., Weiss, S.M., 2015. Porous silicon ring resonator for compact, high sensitivity biosensing applications. Optics Express 23 (6), 7111–7119.
Roth, D.J., Krasavin, A.V., Wade, A., *et al.*, 2017. Spontaneous emission inside a hyperbolic metamaterial waveguide. ACS Photonics 4 (10), 2513–2521.
Salter, P.S., Jesacher, A., Spring, J.B., *et al.*, 2012. Adaptive slit beam shaping for direct laser written waveguides. Optics Letters 37 (4), 470–472.
Schmidt, R., Kaminow, I., 1974. Metal-diffused optical waveguides in linbo3. Applied Physics Letters 25 (8), 458–460.
Soref, R., Lorenzo, J., 1985. Single-crystal silicon: A new material for 1.3 and 1.6 μm integrated-optical components. Electronics Letters 21 (21), 953–954.
Soref, R., Bennett, B., 1987. Electrooptical effects in silicon. IEEE Journal of Quantum Electronics 23 (1), 123–129.
Turbadar, T., 1959. Complete absorption of light by thin metal films. Proceedings of the Physical Society 73 (1), 40.
Vlasov, Y.A., McNab, S.J., 2004. Losses in single-mode silicon-on-insulator strip waveguides and bends. Optics Express 12 (8), 1622–1631.
Wang, C., Xiong, X., Andrade, N., *et al.*, 2017. Second harmonic generation in nano-structured thin-film lithium niobate waveguides. Optics Express 25 (6), 6963–6973.
Wang, C., Zhang, M., Chen, X., *et al.*, 2018a. Integrated lithium niobate electro-optic modulators operating at cmos-compatible voltages. Nature 562 (7725), 101–104.
Wang, C., Zhang, M., Stern, B., Lipson, M., Lončar, M., 2018b. Nanophotonic lithium niobate electro-optic modulators. Optics Express 26 (2), 1547–1555.
Wei, H., Krishnaswamy, S., 2017. Polymer micro-ring resonator integrated with a fiber ring laser for ultrasound detection. Optics Letters 42 (13), 2655–2658.
Weis, R., Gaylord, T., 1985. Lithium niobate: summary of physical properties and crystal structure. Applied Physics A 37 (4), 191–203.
Wood, R., 1902. Xliv. a suspected case of the electrical resonance of minute metal particles for light-waves. A new type of absorption. The London, Edinburgh, and Dublin Philosophical Magazine and Journal of Science 3 (16), 396–410.
Wu, J., Bo, S., Liu, J., *et al.*, 2012. Synthesis of novel nonlinear optical chromophore to achieve ultrahigh electro-optic activity. Chemical Communications 48 (77), 9637–9639.
Wu, Q., Zhang, X.-C., 1996. Ultrafast electro-optic field sensors. Applied Physics Letters 68 (12), 1604–1606.

Wuytens, P.C., Skirtach, A.G., Baets, R., 2017. On-chip surface-enhanced raman spectroscopy using nanosphere-lithography patterned antennas on silicon nitride waveguides. Optics Express 25 (11), 12926–12934.
Xia, F., Mueller, T., Lin, Y.-M., Valdes-Garcia, A., Avouris, P., 2009. Ultrafast graphene photodetector. Nature Nanotechnology 4 (12), 839–843.
Yablonovitch, E., 1987. Inhibited spontaneous emission in solid-state physics and electronics. Physical Review Letters 58 (20), 2059.
Yablonovitch, E., Gmitter, T., Meade, R., *et al.*, 1991. Donor and acceptor modes in photonic band structure. Physical Review Letters 67 (24), 3380.
Yang, Y., Chen, K., Jin, W., Chiang, K.S., 2015. Widely wavelength-tunable mode converter based on polymer waveguide grating. IEEE Photonics Technology Letters 27 (18), 1985–1988.
Ye, S.-W., Yuan, F., Zou, X.-H., *et al.*, 2016. High-speed optical phase modulator based on graphene-silicon waveguide. IEEE Journal of Selected Topics in Quantum Electronics 23 (1), 76–80.
Ye, X., Liu, S., Chen, Y., Zheng, Y., Chen, X., 2020. Sum-frequency generation in lithium-niobate-on-insulator microdisk via modal phase matching. Optics Letters 45 (2), 523–526.
Yu, M., Desiatov, B., Okawachi, Y., Gaeta, A.L., Lončar, M., 2019. Coherent two-octave-spanning supercontinuum generation in lithium-niobate waveguides. Optics Letters 44 (5), 1222–1225.
Zhang, S., Fan, W., Panoiu, N., *et al.*, 2005. Experimental demonstration of near-infrared negative-index metamaterials. Physical Review Letters 95 (13), 137404.
Zhang, Z., Zhao, P., Lin, P., Sun, F., 2006. Thermo-optic coefficients of polymers for optical waveguide applications. Polymer 47 (14), 4893–4896.
Zhao, H., Clemmen, S., Raza, A., Baets, R., 2018. Stimulated raman spectroscopy of analytes evanescently probed by a silicon nitride photonic integrated waveguide. Optics Letters 43 (6), 1403–1406.
Zhao, Q., Cui, K., Feng, X., *et al.*, 2015. Low loss sharp photonic crystal waveguide bends. Optics Communications 355, 209–212.